Manganite/Alq3 interfaces investigated by impedance spectroscopy technique

M. Barra [a,*], A. Cassinese [a], P. D'Angelo [a], L.E. Hueso [b,1], P. Graziosi [b], V. Dediu [b]

[a] CRS COHERENTIA, CNR-INFM and Dipartimento Scienze Fisiche, Università di Napoli ''Federico II'', Piazzale Tecchio 80, 80125 Naples, Italy

[b] ISMN – Istituto per lo Studio dei Materiali Nanostrutturati (CNR), via Gobetti 101, 40129 Bologna, Italy

abstract

With the general objective of studying interfaces between ferromagnetic materials and organic semiconductors, we report ac impedance investigations on $La_{0.7}Sr_{0.3}MnO_3$ (LSMO)/tris(8-hydroxyquinoline)aluminum (Alq_3)/Al and Indium Tin Oxide (ITO)/Alq_3/Al heterostructures, in the frequency range between 20 Hz and 1 MHz. The comparison of the equivalent circuits deduced to fit the experimental ac responses allows isolating a specific RC contribution which can be attributed to the LSMO/Alq3 interface region. Using the information obtained from our ac measurements, we propose a model which fits the temperature dependence of the magnetoresistance in spin valves combining LSMO electrodes

and Alq3 layers.

* Corresponding author. Tel.: +39 0 817682548, fax: +39 0 812391821.
E-mail address: mbarra@na.infn.it (M. Barra).
1 Present address: EC Stoner Lab, Department of Physics and Astronomy,
University of Leeds, LS2 9JT Leeds, United Kingdom.

Letter

Devices based on the combination of the highly spin polarized manganite LSMO and organic semiconductors have recently become the object of great interest and intense research [1,2]. Multilayer structures, where an organic thin film is sandwiched between LSMO and another ferromagnetic electrode (usually Cobalt), exhibit a spin valve effect as a function of the electrode magnetization orientation. At cryogenic temperatures and for low magnetic fields, magnetoresistance (MR) values up to some tens per cent have been demonstrated [2–6]. Room temperature magnetoresistive responses have been also reported [6]. Furthermore, under the application of high magnetic field (>1 Tesla), large negative MR effects have been found in LSMO based organic diodes, even when a non ferromagnetic metal (i.e. Al) is used as top electrode [2,7]. This effect was suggested to be basically related to the carrier injection process from LSMO to the organic layer. Finally, first evidences of electrically addressable non volatile memory effects in LSMO based organic spin valves have been reported [8], opening the perspective to the design of multifunctional devices based on the occurrence of two distinct and non-related physical phenomena. Commonly, most of these interesting features are believed to be strongly affected by the unusual and still not well understood properties of the interface between LSMO and organic layers, where both charge and spin injection occur. Nevertheless, so far, very few studies on the nature of this type of interface have been performed [9].

In this letter, complex impedance spectra of LSMO/Alq$_3$/Al and ITO/Alq$_3$/Al structures from 20 Hz to 1 MHz and in the temperature range between 293 K and 35 K are reported. In recent years, impedance spectroscopy has showed to be a powerful tool to investigate the behavior of multilayer devices, disclosing the contributions of the different layers and the related interfaces [10,11]. The structure of the investigated devices is depicted in Fig. 1a. Glass substrates covered with 120 nm thick ITO patterned strips were used for ITO based devices. LSMO films (40 nm thick) were grown by pulsed electron deposition (pulsed plasma enhanced configuration – PPD) on SrTiO3 substrates, through a shadow mask with a width of approximately 1 mm. LSMO films grown by PPD have been extensively investigated [9,12], showing typical room temperature

conductivity of 102 S/cm and Curie Tc temperatures of about 340 K. Magnetic properties of LSMO films were checked by Magneto-Optical Kerr Effect (MOKE) and found to be in accordance with the existing literature. For any evaporation run, one ITO and one LSMO sample were introduced together in the chamber after a rinse in acetone and isopropanol ultrasonic bath. Before the deposition, the samples were annealed following the procedures established by XPS investigations [12], in order to remove the surface carbon contamination and to restore the surface oxygen stoichiometry in LSMO films. Then, 80 nm thick Alq3 (SIGMA–ALDRICH) films were deposited on ITO and LSMO substrates at room temperature, by sublimation from a Knudsen cell at 10^8 to 10^9 mbar and growth rate of 0.1–0.2 Å/s. Finally, Al films (60 nm thick) were evaporated on the top of Alq3 by using a shadow mask to obtain the final crossbar structure. The device area was 1 mm^2 and, hence, all the reported magnitudes are referred to this value.

Impedance spectra were collected in vacuum by an Agilent LCR meter, mounting the samples in a cryogenic probe station or in a closed cycle cryo-generator equipped with RF probes [13,14]. The oscillating voltage in measuring process was fixed at 100 mV, in order to test the device response in the injection limited current regime where MR phenomena are usually investigated [8]. We have focused on Alq3, since, so far, the combination LSMO/Alq3 showed to provide the most interesting results in organic spintronics, even if an exhaustive explanation for this occurrence is still lacking. Furthermore, the widely investigated behaviour of ITO/Alq3/Al devices, which were used in many cases to analyze the Alq3 intrinsic electrical parameters, represents a reliable reference to evidence the features related to the LSMO/Alq3 interface [11,15–18].

Room temperature real and imaginary parts of the complex impedance, $Z(f) = R(f)+j\chi$ (f) for two typical ITO/Alq3/Al and LSMO/ALq3/Al structures are shown in Fig. 1b and c, respectively. The inset in Fig. 1c represents the same curves in a log–log Nyqvist plot. For both structures, R(f) spectra stay constant in the low frequency range even if at different values. Then, R(f) begin to decrease rapidly as frequency is increased. The corresponding _3 dB cut-off frequencies are 400 Hz and 3.5 KHz for LSMO and ITO based devices, respectively. These differences are also reflected in the position of local maxima in -χ (f) spectra. The non zero values of R(f) in the upper frequency edge reveal a limiting resistance Rs, which has been

estimated to be 300 Ohm for ITO structures and about 5 KOhm for LSMO ones. For comparison, it is clear that the distinguishing features of the LSMO/Alq3/Al device can only be ascribed to the peculiar properties due to the combination between LSMO and Alq3.

With the aim to better address this fundamental issue, the equivalent circuits in the inset in Fig. 1b have been considered to fit the experimental impedance measurements. The fitting curves are also reported in Fig. 1b and c. As shown, the ITO device ac response is well fitted by a single circuit, involving a parallel resistor R_1 and a capacitor C_1, with the Rs in series. This description is in agreement with previous studies, where the ITO/Alq3/Al response has been investigated also as function of temperature and applied bias voltages [15–18]. In our case, R_1 (coinciding with R(f) value at low frequencies) is about 200 KOhm and the extracted equivalent conductivity ($4 \cdot 10^{-9}$ S/cm) is very close to the data reported in Ref. [15].

On the contrary (see the dashed lines in Fig. 1b and c), the same equivalent circuit is not suitable to describe the impedance measurements of LSMO/Alq3/Al structures, where, for all investigated devices, the ac response shows a peculiar behavior in the frequency region above 100 KHz. Indeed, both R(f) and -χ (f) spectra exhibit a slope change at high frequencies, so that adding an extra R_2C_2 component (continuous line) to the above discussed equivalent circuit improves considerably the fitting. This slope change is particularly clear in the -χ (f) spectrum which is not sensitive to the value of the in series resistance Rs. For the investigated devices, R_2 was about 1.5 KOhm, while C2 ranged between 180 pF and 210 pF. By comparison with the ITO device, it comes out the conclusion that the R_2C_2 component has to be attributed to the specific electrical properties of the interface region between LSMO and Alq3.

It seems clear that, despite the nominally similar work function values (4.8–4.9 eV), ITO and LSMO form considerably different interface regions with Alq3. Once again, this experimental evidence confirms that the simple energy barrier heights, coming from the energy gap between the clean electrode work function and the molecular HOMO or LUMO values, offer only a simplified scenario to describe the electrical properties of every specific interface.

The alignment of the energy levels at both ITO/Alq3 and LSMO/ALq3 interfaces has been recently investigated by X-ray (XPS) and ultraviolet

(UPS) photoemission spectroscopy studies [19,9]. These accurate analysis disclosed the occurrence of a significant vacuum level shift (0.9 eV) between LSMO and Alq3, indicating the presence of a strong interface dipole. On the contrary, the same effect is much more limited for ITO/Alq3 interface, where the dipole strength is only 0.1 eV. Considering the annealing procedure followed for our LSMO films before the deposition of the organic film [12], we are able to rule out that the LSMO/Alq3 dipole is due to extrinsic effects such as a contamination layer or unwanted chemical reactions [20]. Although the occurrence of large interface dipoles between organic and conducting electrodes seems to be a general feature of many interfaces, their physical origin is still widely debated in literature and many intrinsic factors (charge transfer, orientation of permanent dipoles, band bending, i.e.) have been invoked to provide an explanation for this phenomenon [21]. To this regard, as far as Alq3 is concerned, the specific polar properties of the molecule have usually been cited to justify its widespread capability to produce interface dipoles. Recent experiments seem to prompt a basic scenario where a density of intermediate states, energetically localized between the electrode Fermi level and the Alq3 LUMO, is induced by the presence of the interface local dipoles [22]. More specifically, a direct relation between the interface states energy distribution parameters and the disorder level of the dipole layer was also found. This occurrence has been demonstrated to strongly affect the charge injection process in the related devices, with the supposed possibility to generate even different conducting states as a function the applied electric field [23].

Despite the agreement with many experimental studies, further research is needed to develop this general theoretical framework and to clarify, in particular, the role of the specific electrode surface electronic properties in affecting the dipole formation and its strength. Recent models suggest that the interface states induction can be considerably mediated by the density of states near the Fermi level of the considered electrode [24]. Although further investigations are required, we believe the R_2C_2 contribution is the electrical representation of the interface charge distribution and the consequent local field related to the interfacial dipole. This result reflects the importance of ac conductivity measurements as a new way of investigating interface physics. Depending on the sample, R1 parameter values range between 400 KOhm and 900 KOhm for LSMO devices, thus resulting always larger than the

values evaluated for ITO devices. Independent DC measurements (not shown here) confirm this result. Similarly C1 values (between 350 pF and 400 pF) in LSMO devices are higher than that deduced for ITO devices (220 pF).

In order to further examine the electrical properties of the interface between LSMO and Alq3, impedance spectra of the LSMO/Alq3/Al devices have been also recorded at different temperatures between 295 K and 35 K. These measurements reported in Fig. 2a and b evidence the different temperature dependences in the low and high frequency range, where the contribution of series resistance Rs and of R_2C_2 component become dominant. To clarify the specific temperature dependence of the various components, the experimental curves have been fitted by the equivalent circuit at any investigated temperature.

Fig. 3 reports the obtained R_1 and R_2 temperature dependence, while the log–log Nyqvist plot of the experimental impedance spectra between 100 KHz and 1 MHz and the corresponding fitting curves is shown in the inset in Fig. 3. Interestingly, the data reveal the complementary behavior of R_1 and R_2. The former follows a semiconducting trend and its value increases up to 5 MOhm at cryogenic temperatures, supporting the idea that R1 is mainly related to the organic film electrical properties. On the contrary, R_2 temperature dependence is metallic-like and its value is about 400 Ohm at 35 K. A complementary behavior is also followed by C_1 and C_2, since the former decreases of 30% from room temperature to 35 K and the latter tends to increase of about 20% in the same range.

Following the basic assumption of the proposed circuit geometry (see Fig. 1b), the R_2C_2 component is related to the electrical properties of the interface region between LSMO and Alq3. The metallic-like temperature dependence of the parameter R2 is apparently quite surprisingly and, so far, there are not any available models able to explain it. Nevertheless, such behavior has been reported in many LSMO based devices, both fully inorganic [25,26] and organic–inorganic devices. Just as an example, it has been found that LSMO/polymer based organic light-emitting diodes showed metallic-like temperature behavior [27], while the light emission was proportional to the electrical current, thus ruling out the short circuits occurrence. While additional investigations are required in order to reveal the basis of this behavior, we can speculate on the influence of the peculiar band structure of the manganite close to the Fermi level. As the metallic

character of LMSO is strongly increased when the temperature is reduced, it is expected to lead to considerably higher injection efficiency at low temperatures. At higher temperatures, the metallic characteristics become increasingly complicated as the metal-insulator transition is approached at around 340 K. Focusing on this subject, it is to remember that the temperature dependence of the spin valve effect has not been satisfactorily explained so far. Usually, MR values decrease drastically with temperature and the phenomenon is explained by invoking the corresponding LSMO superficial magnetization reduction. Fine details are elusive and, up to date, the question seems still open. To this regard, in Fig. 4, we compare our experimental MR temperature dependence (symbols) with LSMO superficial magnetization variation with temperature (dashed line), as obtained from existing literature, in particular from the seminal paper of Park et al., in which magnetization in the superficial 5 Å of a LSMO film was measured by spin-resolved photoemission spectroscopy [28]. Although the superficial magnetization data is indeed coming from a different sample, this kind of behavior is accepted in the community. As shown, the quantitative agreement between both trends is very poor.

In the attempt to overcome this limitation and motivated by recent theoretical studies suggesting the direct proportionality relation between the spin injection efficiency and the interfacial conductivity in manganite/organic systems [29], we tentatively present here a phenomenological model where the interface effect is combined with LSMO magnetization to explain the MR behavior with temperature. To this end, the implicit basic assumptions that both the spin diffusion time inside the organic and the spin injection efficiency of the Cobalt electrode decrease very weakly with temperature in the interval studied [4], are reasonably satisfied.

Then, magnetoresistance MR_{th} temperature dependence has been directly expressed by $MR_{th} = M_{sup} \_ G_{int}$, where M_{sup} is LSMO superficial magnetization and G_{int} is the interfacial conductance given by $1/R_{2N}$. Here, R_{2N} is the LSMO/Alq3 interfacial resistance normalized at T = 20 K, as extracted from R2 data in Fig. 3. R1 is not taken into account in the model, since, as we have demonstrated above, it represents a contribution coming from the bulk of the organic semiconductor. The theoretical MR_{th} data (solid line) calculated by our model are also plotted in Fig. 4. Although this very simple model cannot aim to contain all the

relevant and complex physics of spin injection from manganites into organic semiconductors, the good quantitative agreement between experimental and predicted MRth data obtained in this case confirms the importance of the interfacial resistance in the interpretation of magnetoresistance data for organic spin valves.

In summary, the electrical properties of the LSMO/Alq3 interface region were investigated by comparing impedance measurements on ITO/Alq3/Al and LSMO/Alq3/Al devices. The presence of an interfacial resistance is associated with the interfacial dipole between LSMO and Alq3. The temperature dependence of this resistance evidences the complex character of the half-metal/organic hybrid systems and gives some indication of the critical issues for the development of organic spintronics. In this line, a simple model is presented to show how this occurrence affects the final magnetoresistance response of LSMO/Alq3 hybrid structures. Further studies, in which the intrinsic molecular dipole and hence the interfacial resistance could be modified by deposition parameters, are envisaged.
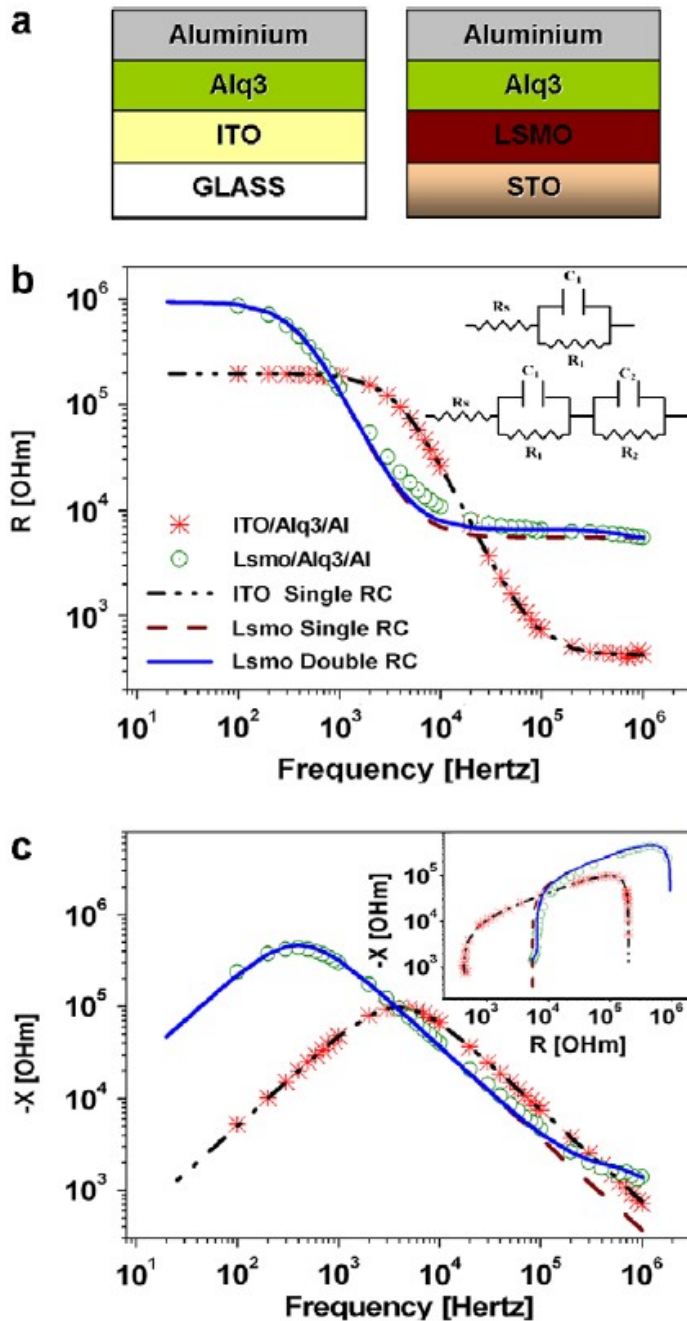
Fig. 1. (a) Structure of the investigated devices, (b) real and (c) imaginary parts of the complex impedance of ITO/Alq3/Al and LSMO/Alq3/Al devices, compared with the fitting curves obtained by the equivalent circuits in the inset in Fig. 1b. In the inset in Fig. 1c, the impedance spectra are reported in a log–log Nyqvist plot.
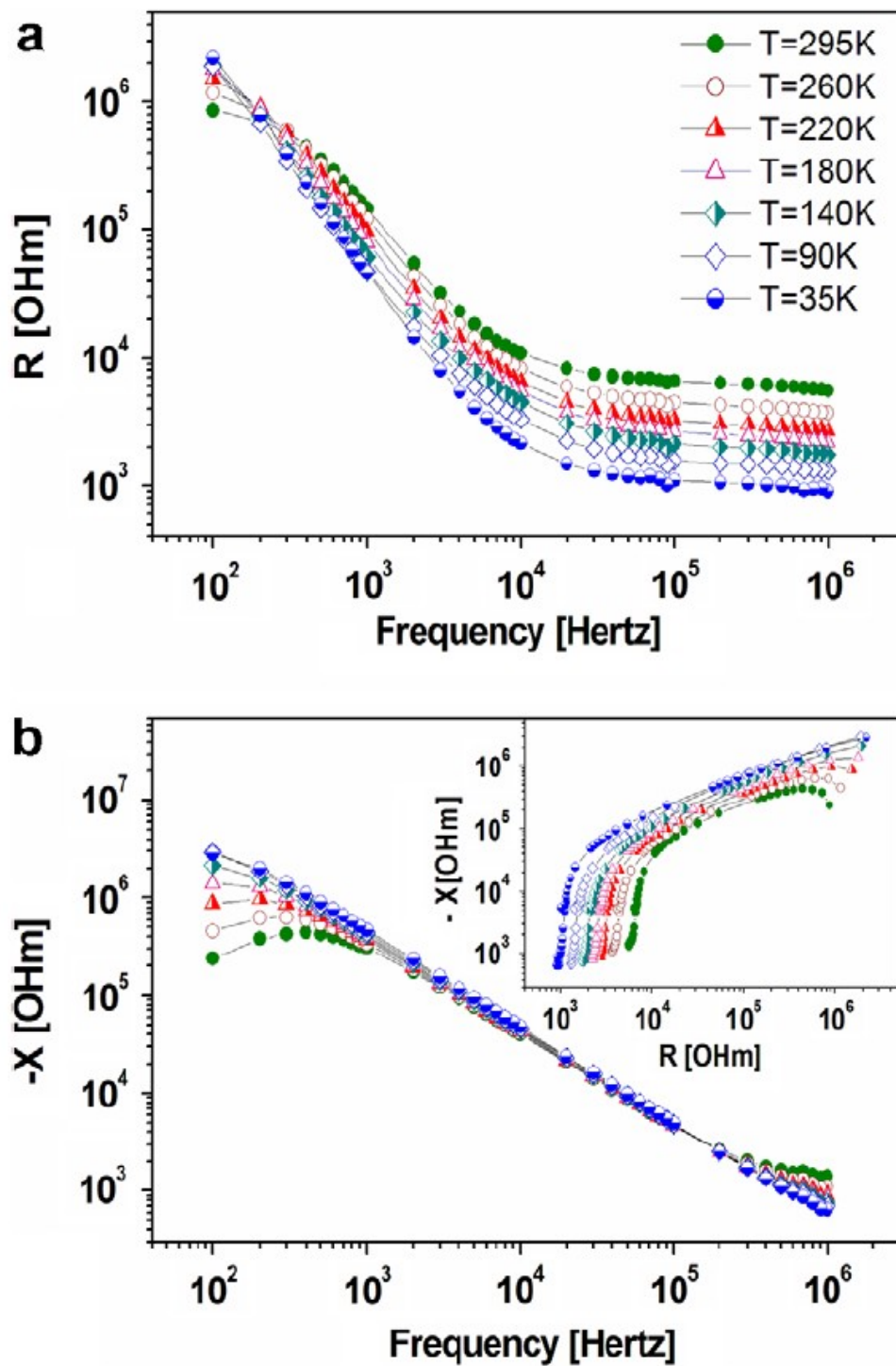
Fig. 2. (a) Real and (b) imaginary parts of impedance spectra recorded for LSMO/Alq3/Al device at different temperatures. In the inset in Fig. 2c, the same spectra are reported in a log–log Nyqvist plot.
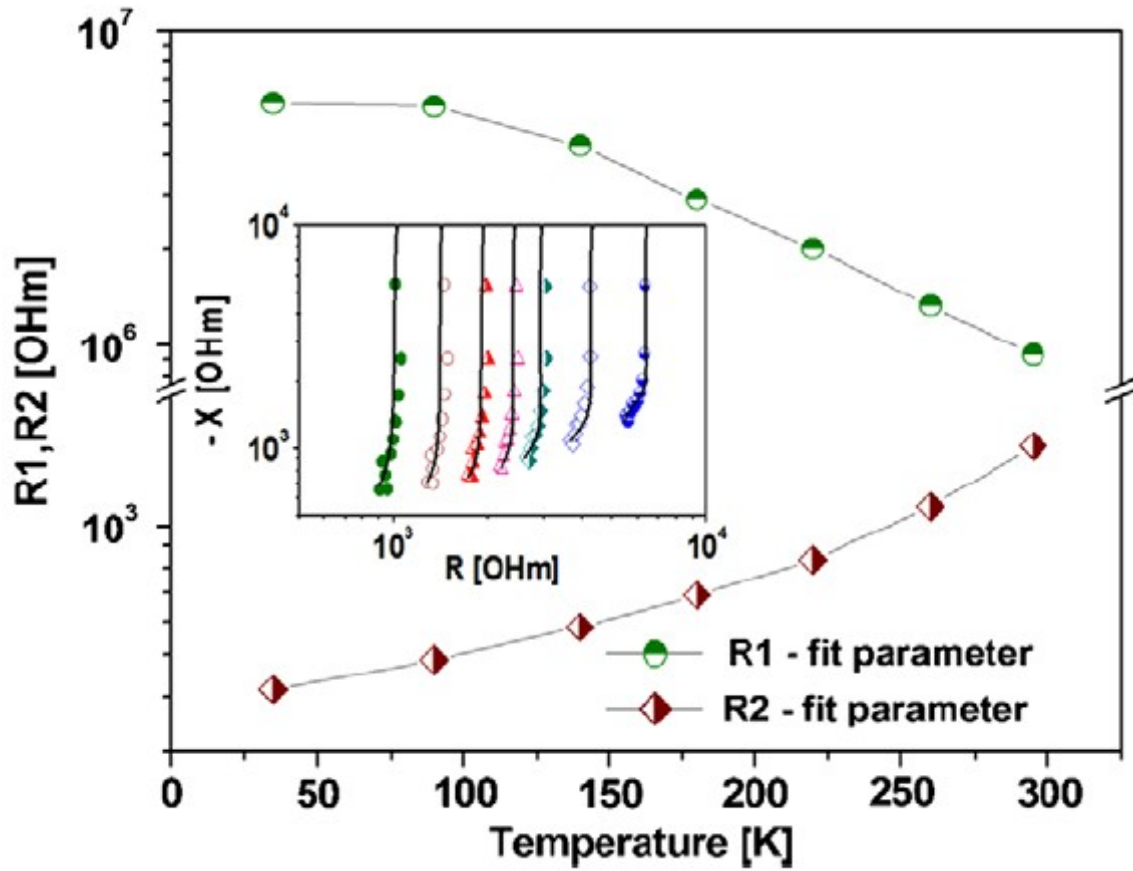
Fig. 3. Temperature dependence of R1 and R2 for LSMO/Alq3/Al equivalent circuit. In the inset, high frequency impedance spectra (symbols) and fitting (solid) curves are reported in a log–log Nyqvist plot.
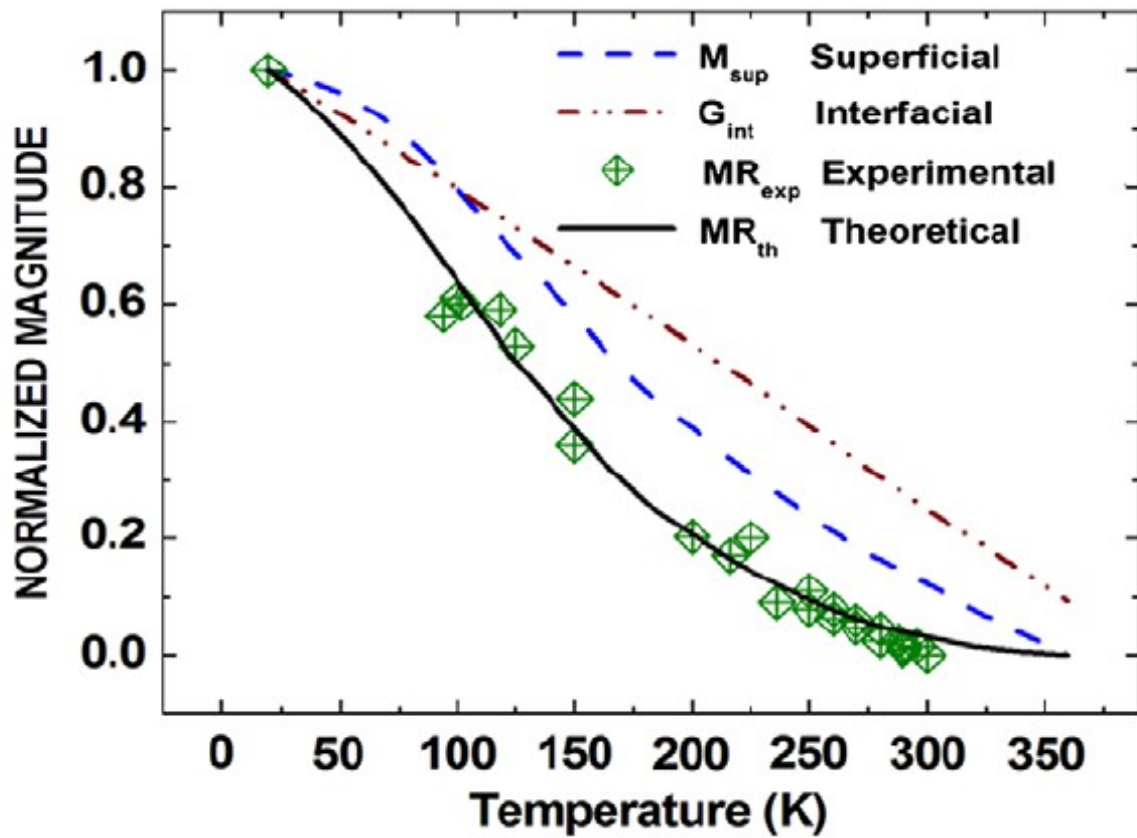
Fig. 4. Experimental (symbols) MR temperature dependence compared with the theoretical data (solid line) calculated by multiplying superficial magnetization M_{sup} (dashed line, Ref. [28]) with the normalized interfacial conductance G_{int} (dash dot line).

Acknowledgement

References

[1] V. Dediu, M. Murgia, F.C. Matacotta, C. Taliani, S. Barbanera, Sol. State Commun. 122 (2002) 181.
[2] Z.H. Xiong, Di Wu, Z.V. Vardeny, J. Shi, Nature 427 (2004) 821.
[3] A. Riminucci, I. Bergenti, L.E. Hueso, M. Murgia, C. Taliani, Y. Zhan, F. Casoli, M.O. de Jong, V. Dediu, arxiv:cond-mat/0701603.
[4] F.J. Wang, C.G. Yang, X.G. Li, Z.V. Vardeny, Phys. Rev. B 75 (2007) 245324.
[5] W. Xu, G.J. Szulczewski, P. LeClair, I. Navarrete, R. Schad, G. Miao, H. Guo, A. Gupta, Appl. Phys. Lett. 90 (2007) 072506.
[6] S. Majumdar, E. Laiho, P. Laukkanen, I.J. Varrynen, H.S. Majumdar, R. Obsterbacka, Appl. Phys. Lett. 89 (2006) 122114.
[7] D. Wu, Z.H. Kiong, X.G. Li, Z.V. Vardeny, J. Shi, Phys. Rev. Lett. 95 (2005) 016802.
[8] L.E. Hueso, I. Bergenti, A. Riminucci, Y. Zhan, V. Dediu, Adv. Mater. 19 (2007) 2639.
[9] Y.Q. Zhan, I. Bergenti, L.E. Hueso, V. Dediu, M.P. de Jong, Z.S. Li, Phys.
Rev. B 76 (2007) 045406.
[10] J. Mc Donald, E. Barsoukov, Impedance Spectroscopy: Theory, Experiments and Applications, John Wiley & Sons, 2005.
[11] W. Brutting, S. Berleb, A.G. Muckl, Org. Elec. 2 (2001) 1.
[12] M.P. de Jong, V. Dediu, C. Taliani, W.R. Salaneck, J. Appl. Phys. 94 (2003) 7292.

[13] P. D'Angelo, M. Barra, M. Nicodemi, A. Cassinese, J. Appl. Phys. 101 (2007) 044910.

[14] M. Barra, M. Biasiucci, P. D'Angelo, A. Cassinese, A.C. Barone, A. Carella, A. Rovello, J. Appl. Phys. 102 (2007) 093712.

[15] A. Moliton, W. Rammal, B. Lucas, Eur. Phys.: J. Appl. Phys. 33 (2006) 175.

[16] A. Moliton, W. Rammal, B. Lucas, Eur. Phys. J. Appl. Phys. 32 (2005) 95.

[17] J.H. Ahn, J.U. Lee, T.W. Kim, Curr. Appl. Phys. 7 (2007) 509.

[18] V.M. Silva, S.K. Mendiratta, L. Pereira, J. Non-Cryst. Solid 352 (2006) 1652.

[19] A.S. Wan, A.J. Makinen, P.A. Lane, G.P. Kushto, Chem. Phys. Lett. 446 (2007) 317.

[20] M. Grobosh, K. Dorr, R.B. Gangineni, M. Knupfer, Appl. Phys. Lett. 92 (2007) 023302.

[21] H. Ishii, K. Sugiyama, E. Ito, K. SEki, Adv. Mater. 11 (1999) 605.

[22] M.A. Baldo, S.R. Forrest, Phys. Rev. B 64 (2001) 085201.

[23] I. Thurzo, H. Mendez, C. Iacovita, D.R.T. Zhan, Synth. Metals 156 (2005) 1108.

[24] H. Vazquez, F. Flores, A. Khan, Org. Elec. 8 (2007) 241.

[25] M.-H. Jo, N.D. Marthur, N.K. Todd, G. Blamire, Phys. Rev. B 61 (2000) R14905.

[26] Y. Ishii, H. Yamada, H. Sato, H. Akoh, Y. Ogawa, M. Kawasaki, Y. Tokura, Appl. Phys. Lett. 89 (2006) 042509.

[27] A. Hayer, A. Kohler, E. Arisi, I. Bergenti, A. Dediu, C. Taliani, M. Al-Suti, M.S. Kahn, Synth. Metals 147 (2004) 155.

[28] J.H. Park, E. Vescovo, H.J. KIm, C. Kwon, R. Ramesh, T. Venkatesan, Phys. Rev. Lett. 81 (1998) 1953.

[29] J.F. Ren, J.Y. Fu, D.S. Liu, L.M. Mei, S.J. Xie, J. Appl. Phys. 98 (2005) 074503.